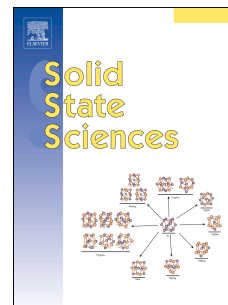


# Accepted Manuscript

High pressure in-situ X-ray diffraction study on Zn-doped magnetite nanoparticles

S. Ferrari, V. Bilovol, L.G. Pampillo, F. Grinblat, D. Errandonea



PII: S1293-2558(17)30897-X

DOI: [10.1016/j.solidstatesciences.2018.01.002](https://doi.org/10.1016/j.solidstatesciences.2018.01.002)

Reference: SSSCIE 5617

To appear in: *Solid State Sciences*

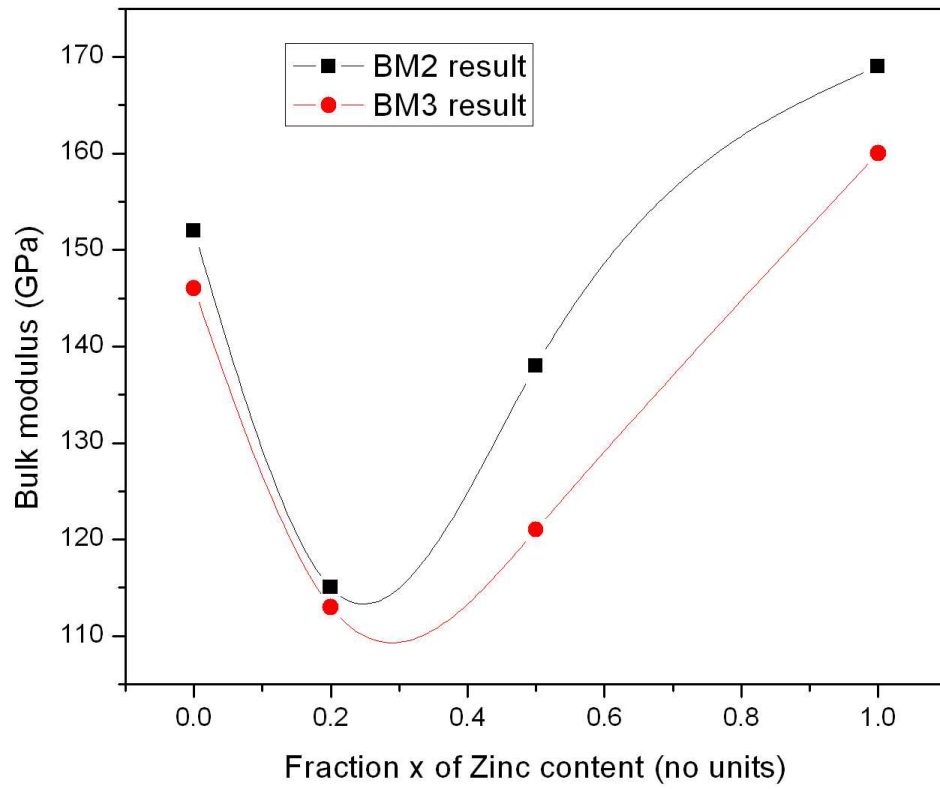
Received Date: 20 September 2017

Revised Date: 7 November 2017

Accepted Date: 3 January 2018

Please cite this article as: S. Ferrari, V. Bilovol, L.G. Pampillo, F. Grinblat, D. Errandonea, High pressure in-situ X-ray diffraction study on Zn-doped magnetite nanoparticles, *Solid State Sciences* (2018), doi: 10.1016/j.solidstatesciences.2018.01.002.

This is a PDF file of an unedited manuscript that has been accepted for publication. As a service to our customers we are providing this early version of the manuscript. The manuscript will undergo copyediting, typesetting, and review of the resulting proof before it is published in its final form. Please note that during the production process errors may be discovered which could affect the content, and all legal disclaimers that apply to the journal pertain.



ACCEPTED

**High pressure in-situ X-ray diffraction study on Zn-doped magnetite nanoparticles**S. Ferrari<sup>1</sup>, V. Bilovol<sup>1</sup>, L. G. Pampillo<sup>1</sup>, F. Grinblat<sup>1</sup>, D. Errandonea<sup>2</sup>

<sup>1</sup> Universidad de Buenos Aires, Consejo Nacional de Investigaciones Científicas y Técnicas, Instituto de Tecnología y Ciencias de la Ingeniería “Ing. Hilario Fernández Long” (INTECIN), Av. Paseo Colón 850, C1063ACV, Ciudad Autónoma de Buenos Aires, Argentina.

<sup>2</sup> Departamento de Física Aplicada –Instituto Universitario de Ciencia de los Materiales, Universitat de València (ICMUV), 46100 Burjassot, Valencia, Spain

**Abstract**

We have performed high pressure synchrotron X-ray powder diffraction experiments on two different samples of Zn-doped magnetite nanoparticles (formula  $\text{Fe}_{(3-x)}\text{Zn}_x\text{O}_4$ ;  $x = 0.2, 0.5$ ). The structural behavior of the nanoparticles was studied up to 13.5 GPa for  $x = 0.2$ , and up to 17.4 GPa for  $x = 0.5$ . We have found that both systems remain in the cubic spinel structure as expected for this range of applied pressures. The analysis of the unit cell volume vs. pressure results in bulk modulus values lower than in both end-members, magnetite ( $\text{Fe}_3\text{O}_4$ ) and zinc ferrite ( $\text{ZnFe}_2\text{O}_4$ ), suggesting that chemical disorder may favor compressibility, which is expected to improve the increase of the Neel temperature under compression.

**1. Introduction**

The system of spinel oxides is a large family of compounds including more than eighty different oxides [1]. These oxides with formulae  $\text{AX}_2\text{O}_4$  have a large variety of technological applications such as high density storage [2], spintronics [3], etc. Magnetite ( $\text{Fe}_3\text{O}_4$ ) has an inverse cubic spinel structure [4], while zinc ferrite ( $\text{ZnFe}_2\text{O}_4$ ), also known as Franklinite, has a normal cubic structure [5]. Solid solutions with general stoichiometry  $\text{Fe}_{(3-x)}\text{Zn}_x\text{O}_4$  ( $x = 0, 0.1, 0.2, 0.5$  and 1) have been investigated previously by us with emphasis on structure and magnetic properties at ambient pressure [6]. The research of spinel oxides under high pressure has gained a considerable attention also due to possible pressure generated changes in physical properties and their applications [7 – 9]. In particular, zinc ferrite squeezed under pressure exhibited superparamagnetism [10].

Despite the fact that there are numerous scientific works on high pressure spinel oxides, most of them are based on bulk specimens and a modest fraction of them treats on nanoparticles. The pressure behavior of nanoparticles is often quite different from bulk materials. In particular, one of the effects seen on nanoparticles is Hall-Petch strengthening [11] (e.g. occurred in other spinel oxide:  $\text{CoFe}_2\text{O}_4$  nanoparticles [12]). Doping a material can also cause changes in the high

pressure performance, as demonstrated in Fe-doped  $\text{SnO}_2$  [13], in doped  $\text{Bi}_2\text{O}_3$  [14], and Ni-doped nanoparticles of  $\text{TiO}_2$  [15].

In this work, we report X-ray powder diffraction high pressure studies performed on Zn-doped magnetite nanoparticles with formula  $\text{Fe}_{(3-x)}\text{Zn}_x\text{O}_4$  ( $x = 0.2$  and  $0.5$ ) to study their compaction under high pressure. The obtained results are compared with a previous study on magnetite ( $x = 0$ ) and zinc ferrite ( $x=1$ ) nanoparticles [16] to test the way the content of Zn affects the compressibility of magnetite nanoparticles.

## 2. Experimental

Zinc-doped magnetite nanoparticles with formula  $\text{Fe}_{(3-x)}\text{Zn}_x\text{O}_4$  ( $x = 0.2$  and  $0.5$ ) were synthesized by wet chemical co-precipitation. The grain size of the particles ranged from 45 to 55 nanometers. The details of the preparation as well as the characterization of the structural and magnetic properties at ambient pressure have been previously reported [6]. Samples of magnetite (of the same batch) and zinc ferrite (synthesized by sol-gel method [6, 16]), with similar grain sizes, were earlier studied by means of X-ray diffraction (XRD) under compression [16].

High pressure powder XRD diffraction experiments were performed at the XDS beam-line of Laboratorio Nacional de Luz Sincrotron (LNLS) located in Campinas, Brazil. High pressure was applied by means of a membrane diamond-anvil cell (DAC). We used stainless-steel gaskets pre-indented to a thickness of 60  $\mu\text{m}$  and diamond-anvils with a culet diameter of 500  $\mu\text{m}$ . The applied pressure was determined by the ruby fluorescence method [17, 18] with an accuracy of 1% in accordance to the most rigorous calibration of the ruby scale [19]. A 4:1 methanol-ethanol mixture, which is quasi-hydrostatic up to 10.5 GPa [20], was used as pressure transmitting medium (PTM). Special attention was paid during sample loading into the DAC in order to avoid sample bridging between diamonds which could strongly affect the result of measurements [21, 22].

XRD experiments were performed in-situ, at room temperature, in the angle-dispersive configuration with a monochromatic beam with a 110  $\mu\text{m}$  width and a wavelength of 0.6199 Å. The images were collected using a CCD Rayonix 165. The two-dimensional images were integrated to one-dimensional (Intensity vs.  $2\theta$ ) diffraction patterns by using the program FIT2D [23]. In the case of the  $\text{Fe}_{2.8}\text{Zn}_{0.2}\text{O}_4$  sample, six different pressures were applied between 1 and 13.4 GPa, and in the case of the  $\text{Fe}_{2.5}\text{Zn}_{0.5}\text{O}_4$  sample, seven different pressures were applied from 1 to 17.4 GPa. The pressures were limited to these values to reduce the influence of deviatoric stresses and to guarantee the structural stability of the cubic spinel phase. The structural analysis was performed using MAUD [24]. We have used a Birch-Murnaghan [25] equation of state to adjust the data of pressure vs. volume.

### 3. Results

#### a) Sample $\text{Fe}_{2.8}\text{Zn}_{0.2}\text{O}_4$

In Fig. 1 we present the XRD diffraction patterns for the sample  $\text{Fe}_{2.8}\text{Zn}_{0.2}\text{O}_4$ . The analysis of the patterns indicates that most of the peaks that corresponds to the magnetite cubic spinel structure (space group  $Fd\bar{3}m$  [4]). There is also a peak corresponding to the ruby (used to determine pressure), which is identified in the X-ray diffraction pattern. At 9.9 and 13.5 GPa there is a peak originated by the gasket. All the Bragg peaks of the sample shift to the right (up to higher  $2\theta$  position) with pressure as expected due to the decrease of the lattice constant. From the fitting procedures by using MAUD software the lattice parameter and the unit-cell volume of the samples were extracted (see supplementary material).

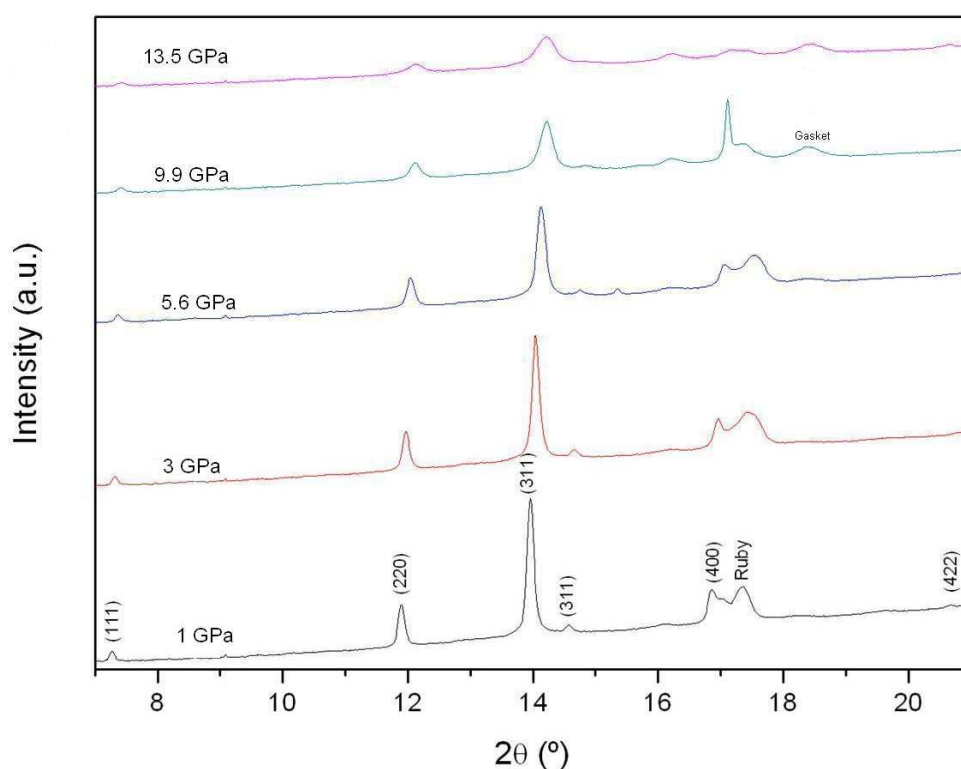


**Figure 1.** X-ray diffraction pattern of  $\text{Fe}_{2.8}\text{Zn}_{0.2}\text{O}_4$  sample at different pressures. The main peaks of the magnetite structure are denoted with the corresponding  $hkl$  values.

The unit-cell volume vs. pressure results are displayed in Fig. 2. The smooth pressure dependence can be represented by a third-order Birch-Murnaghan (BM3) equation of state (EOS),

which was used to adjust the data. Two different regions were considered in the fits: pressures below 10.5 GPa where the pressure-transmitting medium is quasi-hydrostatic, and the complete range of pressure including the measurement at 13.5 GPa where the 4:1 methanol-ethanol mixture is not fully hydrostatic.

The results of fitted EOS curves can be also seen in Fig 2. The adjusted values for the zero-pressure volume ( $V_0$ ), bulk modulus ( $B_0$ ), and its first pressure derivative ( $B_0'$ ) were  $V_0 = 607.2(6) \text{ \AA}^3$ ,  $B_0 = 113(9) \text{ GPa}$ , and  $B_0' = 4.4(5)$  for pressures below than 10.5 GPa; and  $V_0 = 607(1) \text{ \AA}^3$ ,  $B_0 = 117(9) \text{ GPa}$ , and  $B_0' = 3.6(9)$  for all the pressure range. Both sets of parameters agree within the errors. Interestingly, the bulk modulus and its pressure derivative are lower than the measured values for pure magnetite nanoparticles,  $B_0 = 152(9) \text{ GPa}$  and  $B_0' = 5.2(9)$ . They are also below the value of the bulk modulus reported for magnetite, which ranges from 144 to 222 GPa [16]. We compare later systematically the compressibility obtained for same-size nanoparticles of  $\text{Fe}_{2.8}\text{Zn}_{0.2}\text{O}_4$ ,  $\text{Fe}_{2.5}\text{Zn}_{0.5}\text{O}_4$ , magnetite and zinc ferrite.

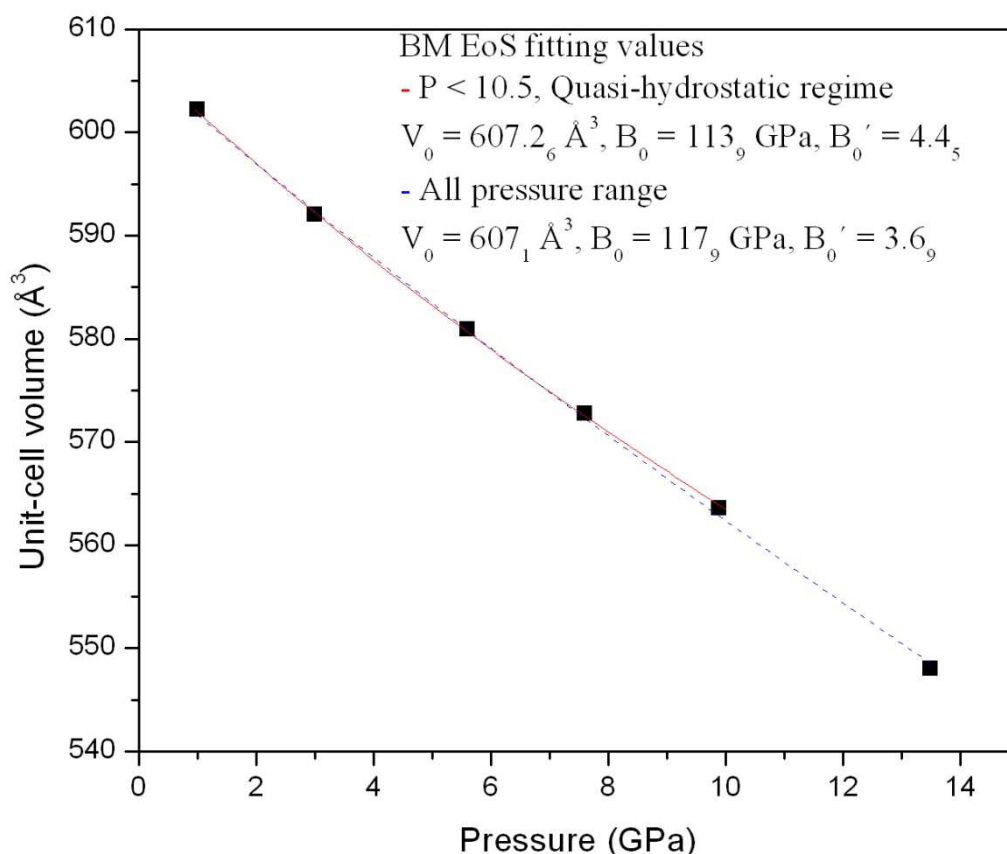


**Figure 2.** Unit-cell volume vs. pressure of  $\text{Fe}_{2.8}\text{Zn}_{0.2}\text{O}_4$  sample. Dots are the experimental values, the solid line is the BM3fit to the data for pressures below 10.5 GPa, and the dashed line is the BM3 fit for all the range.

b) Sample  $\text{Fe}_{2.5}\text{Zn}_{0.5}\text{O}_4$ 

In Fig. 3 we present the XRD patterns of  $\text{Fe}_{2.5}\text{Zn}_{0.5}\text{O}_4$  sample integrated from the corresponding images. Despite the great content of zinc used to prepare this sample, the diffraction peaks can be adjusted to the magnetite cubic spinel structure (space group  $Fd\bar{3}m$ ). Besides, there are peaks corresponding to the ruby present in the DAC. As expected, the peak shift to higher  $2\theta$  values with increasing pressures, indicating the reduction of the cell constant. In the supplementary material, we show a table with the values of cell constant and the unit-cell volume derived from it.

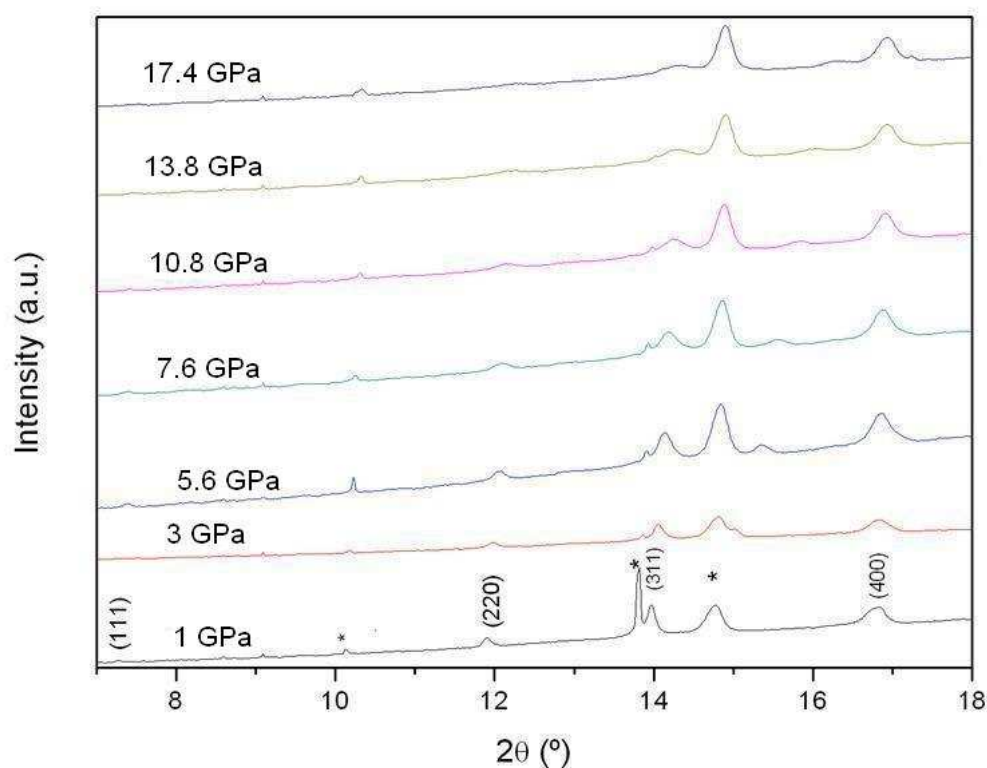


**Figure 3.** X-ray diffraction pattern of  $\text{Fe}_{2.5}\text{Zn}_{0.5}\text{O}_4$  sample at different pressures. The main peaks of the magnetite structure are denoted with the corresponding  $hkl$  indices, the star marks the positions of the ruby diffractions peaks.

Following these data, a third-order Birch-Murnaghan (BM3) equation of state was applied considering as it was employed before two different regions of applied pressures. The data with pressures below 10.5 GPa, where the pressure-transmitting medium is quasi-hydrostatic, and results from the complete range of pressure, including the measurement at 10.8, 13.8 and 17.4 GPa, where the pressure-transmitting medium cannot longer be considered as hydrostatic. The adjusted values

were  $V_0 = 604.0(7) \text{ \AA}^3$ ,  $B_0 = 129(9) \text{ GPa}$ ,  $B_0' = 4.8(5)$  for pressures below than 10.5 GPa; and  $V_0 = 606(1) \text{ \AA}^3$ ,  $B_0 = 125(9) \text{ GPa}$ ,  $B_0' = 4.7(9)$  for the complete pressure range. The values of the bulk modulus and its pressure derivative agree within error bars. On the other hand, they are slightly larger than the values determined for the  $\text{Fe}_{2.8}\text{Zn}_{0.2}\text{O}_4$  sample (which has a lower concentration of zinc). However, the lower limits of the error bars of the values determined for  $\text{Fe}_{2.5}\text{Zn}_{0.5}\text{O}_4$  overlaps with the upper limits of the error bars of the parameters determined for  $\text{Fe}_{2.8}\text{Zn}_{0.2}\text{O}_4$ . This suggests that both doped samples have a similar compressibility [26], which is larger than that of  $\text{Fe}_3\text{O}_4$  and  $\text{ZnFe}_2\text{O}_4$  as we will discuss in the next section.

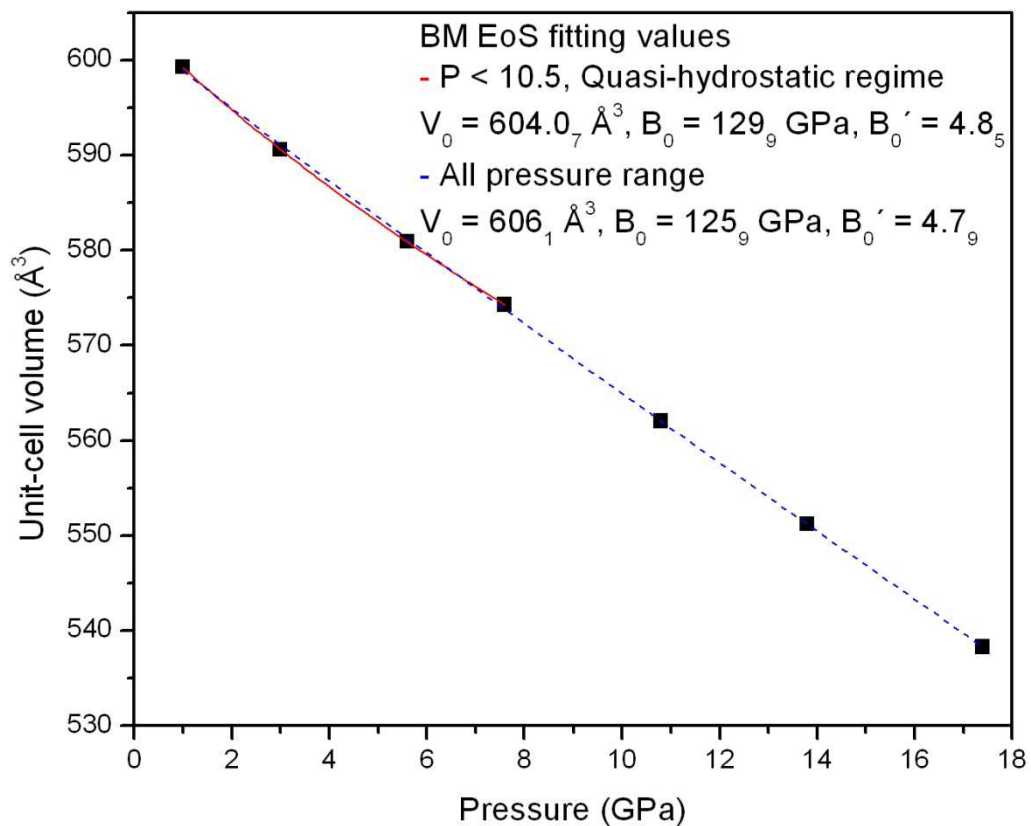


**Figure 4.** Unit-cell volume vs. pressure of  $\text{Fe}_{2.5}\text{Zn}_{0.5}\text{O}_4$  sample. Dots are the experimental values, the solid line is the BM3 fit to the data for pressures below 10.5 GPa, and the dashed line is the BM3 fit for all the measured pressure range.

#### 4. Discussion

Using the results of volume vs. pressure of magnetite and zinc ferrite nanoparticles (of similar grain size) reported previously by us [16] for adjusting a third-order Birch-Murnaghan equation of state, we are able to make a full comparison of the samples with different content of



zinc with general unit formula  $\text{Fe}_{(3-x)}\text{Zn}_x\text{O}_4$  ( $x = 0, 0.2, 0.5$  and  $1$ ). This comparison is resumed in Fig. 5, where the values of bulk modulus and its pressure derivative for the four different Zn compositions.

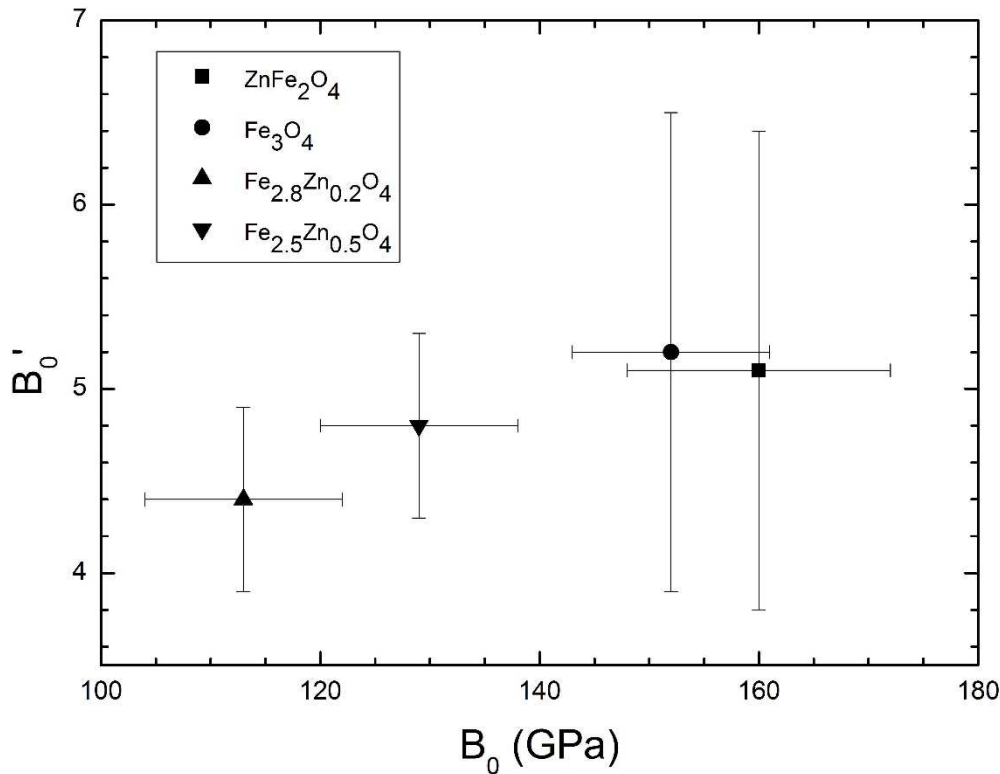


**Figure 5.** Bulk modulus and its pressure derivative  $\text{Fe}_{(3-x)}\text{Zn}_x\text{O}_4$  nanoparticles with a different fraction of zinc content. The values correspond to those obtained using a third-order Birch-Murnaghan EoS. The symbols for different compositions are indicated in the inset.

As it can be seen in the figure,  $\text{Fe}_{2.5}\text{Zn}_{0.5}\text{O}_4$  and  $\text{Fe}_{2.8}\text{Zn}_{0.2}\text{O}_4$  nanoparticles have a bulk modulus which is more than 10% smaller than the bulk modulus of magnetite ( $x = 0$ ) and zinc ferrite ( $x = 1$ ). There is also a tendency for the samples with an intermediate composition to have also a smaller  $B'_0$ , however, for this parameter there is an overlap if the error bars are taken into account. The results summarized in Fig. 5 undoubtedly indicate that  $\text{Fe}_{2.5}\text{Zn}_{0.5}\text{O}_4$  and  $\text{Fe}_{2.8}\text{Zn}_{0.2}\text{O}_4$  are more compressible than the end-members of the family. There are several reasons that can explain this behavior. One is the increase of the volume caused by chemical disorder in  $\text{Fe}_{2.5}\text{Zn}_{0.5}\text{O}_4$  and  $\text{Fe}_{2.8}\text{Zn}_{0.2}\text{O}_4$  [6]. Notice that the volume of these samples is 1-2% larger than that of zinc ferrite and magnetite. Such phenomenon usually induces a reduction of the bulk modulus as

recently found in lanthanide doped  $\text{UO}_2$  [27] and yttrium doped  $\text{Ag}_2\text{S}$  [28]. Other reasonable hypothesis to explain the observed phenomenon is the presence in the doped samples of stoichiometric vacancies in the unit cell as it occurs in spinel sulfides [29] or the enhancement of cation migration under compression in the doped samples [30]. Further studies are needed to establish which of the proposed hypothesis is causing the observed decrease of the bulk modulus in  $\text{Fe}_{2.5}\text{Zn}_{0.5}\text{O}_4$  and  $\text{Fe}_{2.8}\text{Zn}_{0.2}\text{O}_4$ . Of particular relevance to determine the possible cation migration of Zn and Fe are high pressure EXAFS measurements [31], which can be carried out both at the Fe and Zn K-edge. We would like to mention here that the decrease of the bulk modulus for intermediate Zn doping levels suggests a reduction of the cation-oxygen bond stiffness, which should have consequences in many mechanical and vibrational properties and also in transition pressures. Finally, the fact that  $\text{Fe}_{2.5}\text{Zn}_{0.5}\text{O}_4$  and  $\text{Fe}_{2.8}\text{Zn}_{0.2}\text{O}_4$  are more compressible than magnetite and zinc ferrite should have direct consequences in the pressure dependence of the Neel temperature. This temperature is known to increase as the volume of a compound decreases [32]. This suggests that the Neel temperature increase should be enhanced in  $\text{Fe}_{2.5}\text{Zn}_{0.5}\text{O}_4$  and  $\text{Fe}_{2.8}\text{Zn}_{0.2}\text{O}_4$ .

#### 4. Conclusions

In this work, we report a room-temperature powder XRD study on Zn-doped magnetite nanoparticles ( $\text{Fe}_{2.8}\text{Zn}_{0.2}\text{O}_4$  and  $\text{Fe}_{2.5}\text{Zn}_{0.5}\text{O}_4$ ) under compression using synchrotron radiation. The samples used for the experiments were synthesized and characterized at ambient pressure (before high pressure experiments) using a combination of techniques. We determined the effect of pressure in the cubic spinel structure and a pressure-volume EoS for their different Zn-doped systems. None of the samples undergoes a phase transition in the pressures measured. For both samples we have determined that obtained bulk modulus is lower than that of magnetite and of zinc ferrite [16]. We propose possible reasons for the observed decrease in compressibility and discuss potential consequences of such phenomenon. More studies are needed to determine if a similar phenomenon exists in other doped spinel oxides.

#### Acknowledgments

All authors would like to thank J.C. Apesteguy for the synthesis of the samples. S.F., F.G. and L.G.P. thanks the financial support provided by the Agencia Nacional de Promoción Científica y Tecnológica (ANPCyT) under grant PICT-2012-1730. D. E. thanks the support of Spanish MINECO and European FEDER under Grant No. MAT2016-75586-C4-1-P.

#### References

- [1] M.G. Brik, A. Suchocki, A. Kaminska, *Inorg. Chem.* 53 (2014) 5088.
- [2] S. Xuan, F. Wang, Y. Xiang, J. Wang, J. C. Yua, and K. C.-F. Leung, *J. Mater. Chem.* 20 (2010) 5086–5094.
- [3] E. Mayes, A. Bewick, D. Gleeson, J. Hoinville, R. Jones, O. Kasyutich, A. Nartowski, B. Warne, J. Wiggins, K. K. W. Wong, *IEEE Trans. Magn.* 39 (2003) 623.
- [4] T. F. W. Barth, E. Posnjak, *Zeitschrift Kristallographie* 82 (1925) 325–341.
- [5] K. E. Sickafus, J. M. Wills, and N. W. Grimes, *J. Amer. Ceram. Soc.* 82 (1999) 3279–3292.
- [6] S. Ferrari, J. C. Apesteguy, F. D. Saccone, *IEEE Trans. Magn.* 51 (2015) 2900206.
- [7] S. Rahman et al., *Phys. Rev. B* 95 (2017) 024107.
- [8] E. Greenberg et al., *Phys. Rev B* 95 (2017) 195150.
- [9] W. H. Xu, et al., *Phys. Rev.* 95 (2017) 045110.
- [10] Y. Goto, *Jap. J. Appl. Phys.* 3 (1964) 309.
- [11] C.E. Carlton, P.J. Ferreira, *Acta Mater.* 55 (2007) 3749.
- [12] F. D. Saccone, S. Ferrari, D. Errandonea, F. Grinblat, V. Bilovol, S. Agouram, *J. App. Phys.* 118 (2015) 075903.
- [13] F. Grinblat, S. Ferrari, L.G. Pampillo, F.D. Saccone, D. Errandonea, D. Santamaria-Perez, A. Segura, R. Vilaplana, C. Popescu, *Solid State Sci.* 64 (2017) 91-98.
- [14] A. L.J. Pereyra et al., *J. Phys.: Condens. Matter* 25 (2013) 475402.
- [15] K. Karthik, N.V. Jaya, *J. Alloys Compd.* 509 (2011) 5173-5176.
- [16] S. Ferrari, R.S. Kumar, F. Grinblat, J.C. Apesteguy, F.D. Saccone, D. Errandonea, *Solid State Sci.* 56 (2016) 68-72.
- [17] A. Dewaele, M. Torrent, P. Loubeyre, M. Mezouar, *Phys. Rev. B* 78 (2008) 104102
- [18] H. K. Mao, J. Xu, P.M. Bell, *J. Geophys. Res.* 91 (1986) 4673-4676.
- [19] A.D. Chijioke, W.J. Nellis, A. Soldatov, I.F. Silvera, *Jour. App. Phys* 98 (2005) 114905.
- [20] S. Klotz, J. C. Chervin, P. Munsch, and G. Le Marchand, *J. Phys. D* 42 (2009) 075413.
- [21] D. Errandonea, A. Muñoz, and J. Gonzalez-Platas, *J. Appl. Phys.* 115 (2014) 216101.
- [22] D. Errandonea, *Cryst. Res. Techn.* 50 (2015) 729–736.
- [23] A.P. Hammersley, S.O. Svensson, M. Hanfland, A.N. Fitch, D. Häusermann, *High Press. Res.* 14 (1996) 235.
- [24] L. Lutterotti, M. Bortolotti, G. Ischia, I. Lonardelli, and H.-R. Wenk, *Z. Kristallogr.* 26 (2007) 125.
- [25] F. Birch, *J. Geophys. Res.* 57 (1952) 227.
- [26] O. Gomis, B. Lavina, et al., *J. Phys.: Condens. Matter* 29 (2017) 095401.
- [27] D. R. Rittman, S. Park, et al., *J. Nuclear Mater.* 490 (2017) 28 – 33.
- [28] P. Wang, R. Zhao, et al., *RSC Advances* 7 (2017) 35105 – 35110.
- [29] D. Santamaria-Perez et al., *J. Phys. Chem. C* 116 (2012) 14078–14087.
- [30] D. Errandonea et al., *Physical Review B* 79 (2009) 024103.
- [31] J. Ruiz-Fuertes, A. Friedrich, et al., *Chem. Mater.* 23 (2011) 4220–4226.

### Supplemental Material

Pressure (GPa)	Lattice constant (Å)	Unit-cell volume (Å <sup>3</sup> )
1.0(1)	8.4445(3)	602.18(6)
3.0(1)	8.3967(2)	592.00(4)
5.6(1)	8.3439(3)	580.92(5)
7.6(1)	8.3045(5)	572.7(1)
9.9(1)	8.2602(6)	563.6(1)
13.5(1)	8.1833(6)	548.0(1)

Table 1. Values of lattice constant and unit-cell volume for different pressures of Fe<sub>2.8</sub>Zn<sub>0.2</sub>O<sub>4</sub>

Pressure (GPa)	Lattice constant (Å)	Unit-cell volume (Å <sup>3</sup> )
1.0(1)	8.4307(9)	599.2(2)
3.0(1)	8.3897(5)	590.5(1)
5.6(1)	8.3440(5)	580.9(1)
7.6(1)	8.3118(6)	574.2(1)
10.8(1)	8.2524(6)	562.0(1)
13.8(1)	8.1991(6)	551.2(1)
17.4(1)	8.1344(6)	538.2(1)

Table 2. Values of lattice constant and unit-cell volume for different pressures of Fe<sub>2.5</sub>Zn<sub>0.5</sub>O<sub>4</sub>.

ACCEPTED MANUSCRIPT

- Two samples of Zn-doped (with different stoichiometry) nanocrystals were studied under high pressure.
- Bulk compressibility is determined
- The bulk compressibility is lower than the found values for nanocrystals of magnetite (no Zn doping) and Zinc ferrite (full doping).

ACCEPTED MANUSCRIPT